INTERNATIONAL JOURNAL of RENEWABLE ENERGY RESEARCH
N. K. Pandey et al., Vol.16, No.1, March, 2026

Artificial Rabbit Optimization Based MPPT Technique for PV System Performance Investigation

Nirmal Kumar Pandey*, Rupendra Kumar Pachauri **, Sushabhan Choudhary***, Sudhakar Babu Thanikanti****‡, Sumit Kumar Maitra*****, Ranjana Yadav*****

* Department of Electronics & Communication Engineering, Shivalik College of Engineering, Dehradun, 248197, India.

** Electrical Cluster, School of Advanced Engineering, UPES, Dehradun, 248007, India.

**Miyan Research Institute, International University of Business, Agriculture and Technology, Dhaka-1230, Bangladesh

*** EED, School of Engineering, University of Petroleum and Energy Studies, Dehradun, 248007, India.

**** EED, Chaitanya Bharathi Institute of Technology, Telangana, 500075, India.

****Department of Electrical and Electronics Engineering, Manav Rachna Institute of Research and Studies, Faridabad, Haryana, 121004, India.

*****Department of Chemistry, Ramjas College, University of Delhi, Delhi, India

(nirmalpande84@gmail.com, rpachauri@ddn.upes.ac.in, schoudhury@ddn.upes.ac.in, sudhakarbabu66@gmail.com, sumitmaitra.set@mriu.edu.in,ranjanyadav@ramjas.du.ac.in)

‡ Corresponding Author; Sudhakar Babu Thanikanti, Chaitanya Bharathi Institute of Technology, Telangana, 500075, India, Tel: +91 7382163424, sudhakarbabu66@gmail.com

Received: 13.10.2023 Accepted: 11.12.2023

Abstract- Comprising partial shadowing (PS) conditions, the photovoltaic cells in the array of solar panels get reversed biased and function as a load, resulting in hotspot concerns that can dramatically decrease the photovoltaic's efficiency. The Perturb & Observe (MPPT) technique is typically used in solar systems, but it is highly challenging to recognize the actual maxima when both local maxima and global maxima are present during the PS conditions. The solar PV system's efficiency may be significantly decreased as a result of an innovative approach used in this research that employs artificial rabbit optimization (ARO). In the present research, the GMPP was tracked under PS conditions utilizing the proposed ARO technique in conjunction with additional meta-heuristic algorithms such as PSO, GWO, FPA, and CS. We assess how well different strategies perform in terms of GMPP tracking. The effectiveness, standard deviation (STD), rise time, settling time, mean, root mean square error (RMSE), and median of metaheuristic procedures are evaluated and compared to those of the traditional P&O methodology. The constraints of conventional P&O algorithms are eliminated by a suggested algorithm, which can adapt to quickly changing conditions by collecting numerous peaks. The proposed algorithm's advantage over the traditional P&O technique and most popular metaheuristic algorithms such as PSO, GWO, and FPA is shown through comparison with the latter in terms of accuracy, efficiency, and decreased oscillations. The proposed model reaches an efficiency of roughly 99.98%. Additionally, it has a rising time of about 387.38ms , a settling time of 2.77 s, and a best standard deviation of 13.15.

Keywords Artificial rabbit optimization, partial shading, PV systems, metaheuristic algorithms, global maximum power point.

1. Introduction

In recent years, photovoltaic (PV) systems have gained popularity as a viable renewable energy option. The absence of greenhouse gas emissions from solar energy makes it an invaluable tool in the fight against global warming[1]. Furthermore, PV cell production has become more eco-friendly, resulting in a smaller carbon footprint. In spite of these advantages, researchers in science continue to face an enormous challenge in enhancing the efficacy of photovoltaic (PV) systems as a whole. The inclusion of maximum power point tracking (MPPT) components in these systems is primarily motivated by this consideration. [2] Partially

shading (PS) conditions, where the PV systems are shaded by trees, nearby buildings, or poles, have arisen as a result of the widespread installation of PV systems on building rooftops to meet long-term economic prospects while reducing the overall cost of installation [3]. Given that the system's power-voltage (P-V) graph reveals many localized maximum power points (LMPPs) in addition to one global maximum power point (GMPP) peak under PS conditions, it can be tricky to recognize the proper GMPP for capturing the maximum power [4]. Certain regions of the PV receive ample sunlight and function effectively; nevertheless, shady cells do not, which significantly reduces power generation. To reduce impairments, bypass diodes are incorporated within influenced sections [5]. It is widely acknowledged that the MPP of PV systems relies predominantly on sporadic weather and irradiations as shown in Fig. 1. When a PV array is partially shaded, two LMPPs and one GMPP are present. as shown in Fig. 2. It is well known that partial shading of series-connected PV modules will significantly reduce or increase their capacity, either linearly or nonlinearly [6].

There is a plethora of MPPT techniques described in the literature, most of which fall into one of two categories: conventional and metaheuristic techniques. Considering their simplicity and accuracy in monitoring the MPP under consistent environmental conditions, perturb and observe (P&O) and incremental conductance (IC) are commonly utilized in photovoltaic systems with linear loads, battery management, and grid-connected inverters; however, they are not suitable for use in environments with partial shading [7].

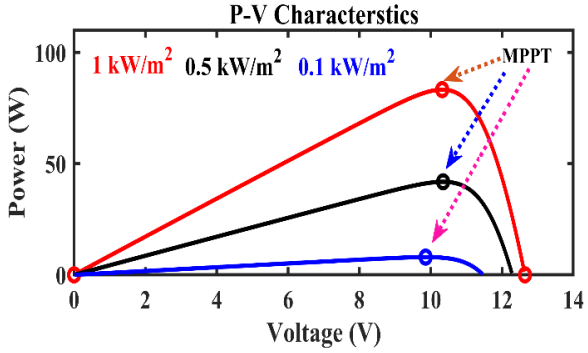

Fig. 1. PV characterstics during normal conditions.

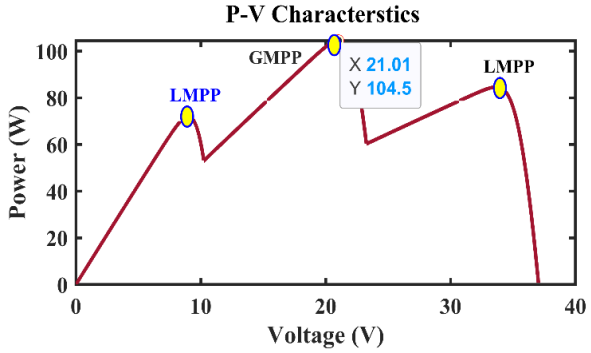

Fig. 2. P-V Characterstics during PS.

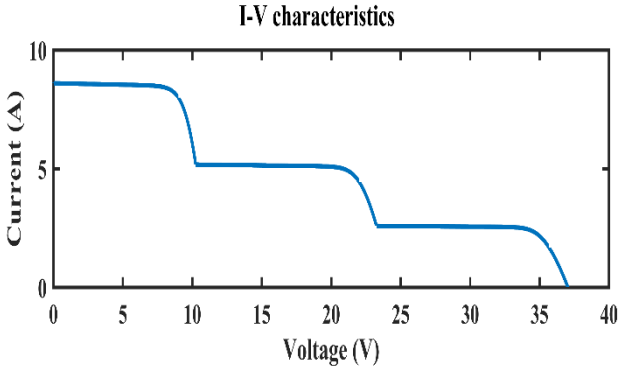

Fig. 3. I-V Charasterstics during PS.

1.1 Motivation

Conventional approaches fall short of tracking the GMPP and instead settle at a LMPP or in the vicinity of the GMPP, which reduces the PV system's overall efficiency [8]. The use of nature-inspired optimization algorithms is becoming more prevalent to solve complex optimization problems [9]. Optimization algorithms are a very powerful and effective method for dealing with nonlinear MPPT challenges caused by PS in photovoltaic systems. Particle swarm optimization (PSO) and ant colony (ACO) are two of the most popular optimization algorithms in MPPT problems, as they provide significant benefits consisting of a lack of knowledge of the system's internal parameters and a lower demand for computation [10]. However, the PSO and ACO algorithms are rigid because they both rely on the identification of control parameters [11]. Additionally, the initial positions of the particles have a significant impact on the PSO's convergence. Recent advances in nature-inspired methods include grey wolf optimization (GWO) [12]. It draws inspiration from the social organization and foraging strategies of grey wolves. The GWO algorithm was found to offer extremely competitive outcomes in comparison to well-known swarm intelligence-based algorithms with regard to outstanding solution reliability, convergence despite the beginning conditions, control clarity, and its ability to manage neighbourhood minima [13]. Moth-Flame optimizations utilize the duty cycle control of the converter as its parameters in order to track the GMPP under PS [14]. For tracking GMPP, a discrete PSO (DPSO) is employed under PS.The classic PSO's randomness and acceleration coefficient elements are eliminated by the DPSO, streamlining the GMPP tracking [15]. For effective tracking of GMPP in PS, a colony of flashing fireflies is used. Both theoretical analysis and empirical evidence show that it excels over conventional approaches like PSO in terms of tracking velocity and PV output power fluctuations [16]. To alter the flying squirrel's location in the absence of a predator, a modified version of Flying Squirrel Search Optimization (FSSO) is suggested [17]. P&O and PSO are outperformed by Cuckoo Search in terms of convergence, transient behaviour, and tracking GMPP [18]. In [19] ant colony optimization (ACO) technique serves as the foundation for the ANN-ACO MPPT controller. It is helpful in training the created ANN and in evolving the connection weights and biases to obtain the ideal duty cycle converter values that correlate to the MPP of

a PV array. İn [20] optimal FOPID is implemented for PV wire feeder systems. [21] represents the implementation of PSO tuned ANFIS controller for MPPT of PV systems. İn [22] the authors implemented active filters for compensation of harmonics and reactive power of a grid connected PV systems.

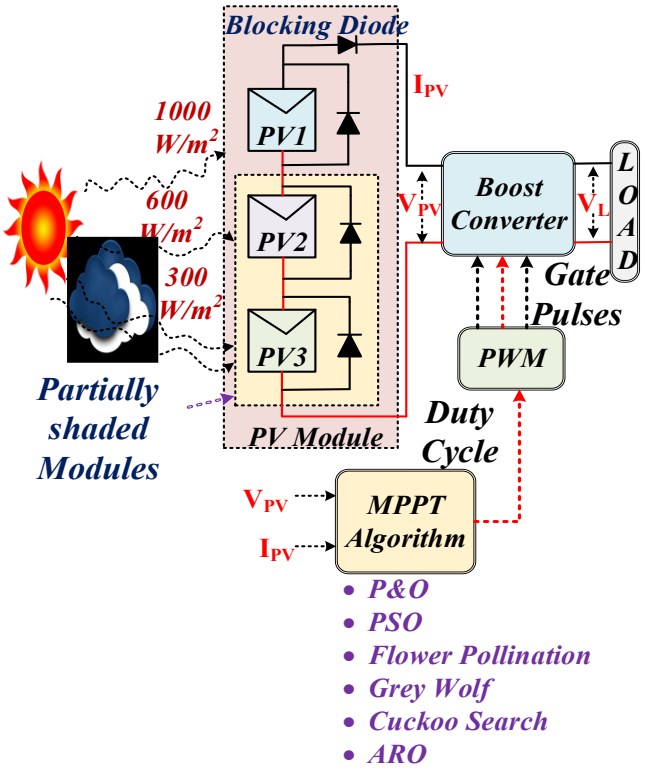

Fig. 4. Proposed system.

1.2 Research Gap

Despite a number of MPPT strategies have been explored in the literature, there is still a need to identify a strategy that monitors the GMPP with the fewest number of iterations and oscillations possible when a partial shading is prevalent. Further developments in MPPT techniques are necessary for PV systems under partial shadowing, as evidenced by the limits of existing algorithms, which include sensitivity to beginning circumstances and dependence on control parameters.

1.3 **Contribution**

For GMPPT of PV systems under partial shadowing situations, a novel MPPT is put out in this study. The artificial rabbit optimization (ARO) that has been proposed tracks the GMPP with fewer iterations, thereby minimizing oscillations near the GMPP and minimizing tracking time. The findings of the suggested method have been compared with those of the traditional P&O MPPT technique, along with PSO, the Cuckoo search algorithm, Greywolf optimization, and flower pollination metaheuristic algorithms.The MATLAB/Simulink platform has been utilized for implementing the recommended technique.

1.4 Paper Organization

The manuscript is organized into five sections, as depicted in Fig. 5 The importance of MPPT in PV systems and the effects of PS conditions are the primary topics of Section 1. The system modelling and its parameters are covered in Section 2. Section 3 focuses mostly on MPPT algorithms, providing the mathematical underpinnings for each algorithm as well as outlining the suggested technique. A thorough examination and insight into the various MPPT approaches are provided in Section 4. The conclusion and comparative analysis of the suggested method based on various parameters are presented in Section 5.

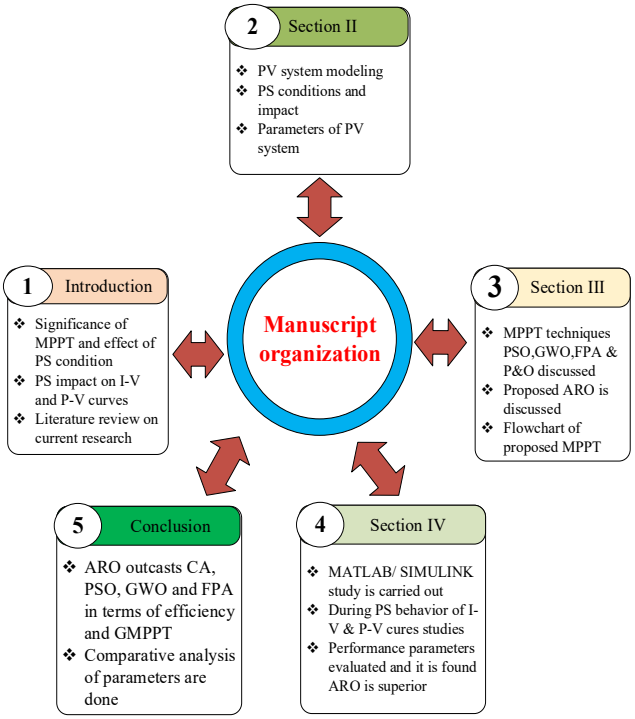

Fig. 5. Manuscript organization.

2. PV System Modelling and the Influence of PS Conditions

The maximum PV output from the solar cells must be attained in order to reach the MPPT criteria. This calls for an analysis of the relationships between voltage and current (I-V), power and voltage (P-V), and other crucial solar cell properties. **Fig. 6** depicts the comparable circuit for the single PV cell.

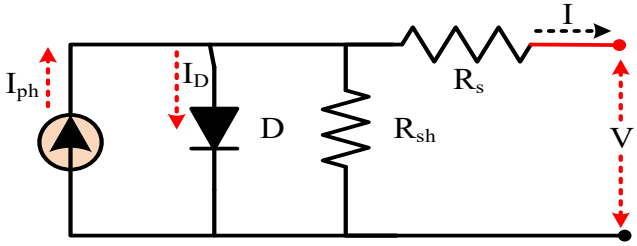

Fig. 6. Equivalent circuit of PV using a single diode.

The equivalent PV system current is calculated using the basic equations derived from the Kirchhoff current rule as

$$I = I_{ph} - I_o\left[e^{\frac{q(V+IR_S)}{KTA}-1}\right] - \frac{V+IR_S}{R_{sh}} \quad (1)$$

Where I represents the output current, V represents the voltage across the PV, and I_{ph}, K, T, A denotes the photocurrent , Boltzmann constant , temperature and ideality factor. R_S and R_{sh} denotes the resies and shunt resistance.

$$I_{ph} = \left(I_{sc} + k_i\Delta T\right)\frac{G}{G_{STC}} \quad (2)$$

$$I_o = I_{oSTC}\left(\frac{T_{STC}}{T}\right)^3 e\left[\frac{qE_g}{AK}\left(\frac{1}{T_{STC}} - \frac{1}{T}\right)\right] \quad (3)$$

$$I_{oSTC} = \frac{I_{sc}}{e\left(\frac{qV_{oc}}{AKT_{STC}}\right)-1} \quad (4)$$

I_{sc} represents the generated current from the PV systems during the standard test conditions (STC), which are defined as a temperature (T) of 25 ºC and irradiance (G_{STC}) of 1000 W/m^2. The energy bandgap is represented as E_g, while k_i is the short-circuit current coefficient. I_{oSTC} denotes the nominal saturation current at STC. Voc is the open-circuit voltage of a solar cell. The PS condition is created in the PV modules by employing three PV modules with a total of 60 solar photovoltaic cells, each with 20 cells. Each of these three models, which are connected in series, has a bypass diode, and by changing the irradiance of each model at a specific value, such as a fixed 1000 W/m^2 for panel 1, 300 W/m^2 for panel 2, and 600 W/m^2 for panel 3. The equivalent model of the connected solar PV system is shown in **Fig. 7**. The parameters of modules are provided in Table 1, while the P-V and I-V characteristics during the PS conditions are depicted by Fig. 2 and 3, respectively.

Table 1. Partially shaded parameters of PV

Parameters	*Values*
No. Of cells in each module	20
MPPT	83.28 W
V_{MPPT}	10.32 V
I_{MPPT}	8.07 A
V_{OC}	12.64 V

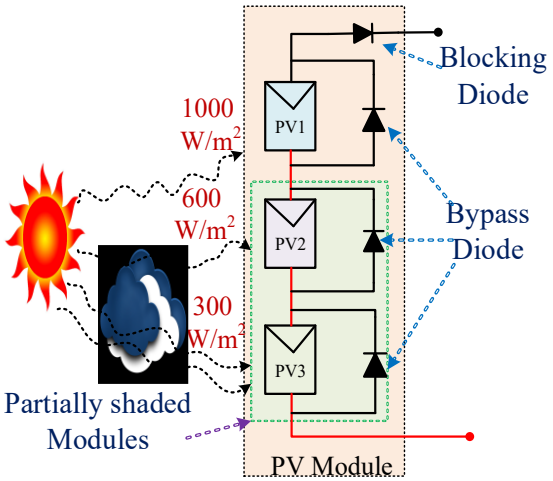

Fig. 7. Partially shaded PV module.

The PS causes a change in the PV array's behavior, leading to reverse biased conditions, power loss, and the formation of possible hotspots because of reduced current production from shaded panels. **Fig. 7** illustrates the PS conditions: panel 1 receives 1000 W/m^2 , while the due to the presence of clouds panel 2 gets 600 W/m^2, and panle 3 receives 300 W/m^2 irridations respectively, leading to the development of hotspots and a correspondingly large drop in power output.

3. MPPT Algorithms

3.1 Perturbation and Observation Method

The P&O approach is frequently employed for MPP tracking. By using this method, a slight disturbance is introduced into the PV module, changing its power output. Regularly testing the power output and comparing the results to previous data are required to determine how well the PV system is operating. If the output power increases, it will carry on as usual; if it decreases, the disturbance will be reversed. During this algorithm cycle, the PV module voltage and the array voltage are modified. The PV module's voltage can be changed upwards or downwards to see if the power has increased or decreased.

3.2 Particle Swarm Optimization

Particle swarm optimization (PSO) is a well-known method of optimization that takes its cues from the cooperative efforts of animals like groups of fish and bird flocks. To identify the best answer, PSO propels a population of particles representing possible answers through the search space [23]. There are two distinguishing features of every particle. This is a position in the search space that could be a potential answer. Typically, the following equations determine the velocity and position updates for each particle. The particle's velocity in the search space indicates its direction and rate of motion.

$$P_i^{t+1} = wP_i^t + c_1r_1(P_{best_i} - Y_i^t) + c_2r_2(G_{best} - Y_i^t) \quad (5)\ [23]$$

$$Y_i^{t+1} = Y_i^t + P_i^{t+1} \quad (6)\ [23]$$

Where P_i^t is the velocity of particlee i, Y_i^t is position of particle at iteration t, P_{best_i} is the best known positions and G_{best} is the best known postion , w is inertia weight , c_1 and c_2 are acceleration coefficients , while r_1 and r_2 are random values between $[0,1]$.

The Fig. 8 shows the velocity and position update of the particles using the PSO. By defining position as the current duty cycle (d) and velocity (V) as the deviation from that value, we can derive an equation describing the converter's duty cycle.

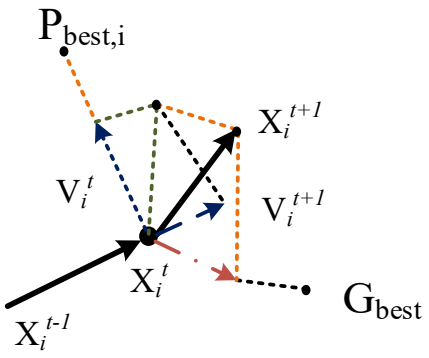

Fig. 8. Veolicty and position update in PSO.

$$d_i^{t+1} = d_i^t + V_i^{t+1} \quad (7)$$

İt is evident from Eq.7 that the duty cycle depends on the P_{best_i} and G_{best} .

3.3 *Flower Pollination Optimization*

The flower pollination process in plants served as the inspiration for the Flower Pollination Algorithm (FPA), a naturalistic optimization system. As a metaheuristic optimization technique, it was developed to address a range of optimization issues. Nature uses both abiotic and biotic methods of pollination. Abiotic pollination just relies on water and wind, whereas biological pollination depends on migrants like birds and insects to move pollen between blooms [24]. The FPA takes into account self- and cross-pollination techniques in addition to biotic and abiotic pollination. Switching probability controls local or global pollination selection. Global pollination occurs if a random number exceeds the switching probability; otherwise, local pollination occurs. The governing equations for the biotic process are described mathematically as Eq.8 - Eq.10.

$$U_i^{t+1} = U_i^t + \gamma L(\lambda)(G_* - U_i^t) \quad (8)$$

$$L(\lambda): \frac{\lambda\Gamma(\lambda)\sin(\frac{\lambda\pi}{2})}{\pi}\frac{1}{d^{1+\lambda}} \quad (9)$$

Where U_i^t represents the solution vector at iteration t, G_* is global solution, γ is scaling factor while $L(\lambda)$ is the levy factor. The abiotic process is described by Eq. 11, and mathematically expressed as

$$U_i^{t+1} = U_i^t + \in (U_l^t - U_k^t) \quad (10)$$

Where U_l^t and U_k^t are the two different pollens froms the plant.

3.4 *Grey wolf Optimization*

The GWO algorithm aligns the proposals of grey wolf leadership and hunting mechanisms. As apex predators, grey wolves prefer packs to simulate leadership responsibilities [25]. To quantitatively model wolf social hierarchy in GWO design, we employ the fittest solution as alpha (α). Consequently, the second and third best answers are beta (β) and delta (δ), respectively. Other possible solutions are considered to be omega (ω). There are three steps to the GWO algorithm: pursuit, wrapping around, and assulting prey. Grey wolves encircle prey during the hunt, which can be approximated by Eqs.11- 12.

$$G = |\, C.Y_p(t) - Y(t) \,| \quad (11)$$

$$Y(t+1) = Y_p(t) - A.G \quad (12)$$

Where A and C denotes the coefficient vectors, Y_p represents the position vector of the prey while Y represents the position vector of the prey. The best solution is updated using the mathematical equations Eq.13- Eq.15.

$$\left.\begin{aligned} G_\alpha &= |\, \vec{C}_1.Y_\alpha - Y \,| \\ G_\beta &= |\, \vec{C}_1.Y_\beta - Y \,| \\ G_\delta &= |\, \vec{C}_1.Y_\delta - Y \,| \end{aligned}\right\} \quad (13)$$

$$\left.\begin{aligned} Y_1 &= Y_\alpha - \vec{A}_1.(G_\alpha) \\ Y_2 &= Y_\beta - \vec{A}_1.(G_\beta) \\ Y_3 &= Y_\delta - \vec{A}_1.(G_\delta) \end{aligned}\right\} \quad (14)$$

$$Y(t+1) = \frac{Y_1 + Y_2 + Y_3}{3} \quad (15)$$

The duty cycle of the converter is goverend by the Eq.16.

$$D_i(t+1) = D_i(t) - A.D \quad (16)$$

3.5 *Cuckoo Search optimization*

The cuckoo search algorithm, which is used for MPPT under PSC, was created using natural inspiration and has its foundation in the spawning process of cuckoo birds [26]. It is based on some cuckoo species' brood parasitism behavior, in which the cuckoos lay their eggs in the nests of other bird species and allow the other birds to nurture their young. This behavior served as the basis for the creation of a search algorithm that imitates the cuckoo's egg-laying and host bird nest rejection processes in order to discover the optimum solution. An essential component of the cuckoo's reproduction strategy is looking for a suitable host bird's nest [27]. The hunt

for a nest typically resembles the hunt for food in that both involve random or nearly random behavior. When in search of food, animals frequently follow paths or trajectories that are representable by particular mathematical functions. The Lévy flight is one of the most prevalent models. A Lévy flight is a random walk where the step sizes are generated from the Lévy distribution. The optial solution is found using Eqs.17- 19.

$$X_i^{(t+1)} = X_i^t + \alpha \oplus \text{Levy}(\lambda) \quad (17)$$

$$\text{Levy}: \ u = t^{-\lambda}, (1 < \lambda < 3) \quad (18)$$

$$X_i^{best} = X_i^t + \alpha(X_{best}^t - X_i^t) \oplus \text{Levy} \quad (19)$$

3.6 Artificial Rabbit Optimization

The proposed ARO's effective optimization model gives a mathematical description of the actual survival tactics used by rabbits in the wild. Detour eating and inadvertent concealment, two methods that are frequently emulated, are therefore examined. An initial simulation of the detour-foraging method is conducted. As part of this tactic, the rabbit is instructed to consume the grass that is present around nearby nests in an effort to hide its own nest from potential predators [24]. The positions of the rabbits are updated after each iteration in accordance with the guidelines of the offered approach, and then they are subjected to an assessment of the objective function. As the process goes on, the agents will get more successful in finding the bunnies' hiding places, which stand in for the solutions. Each member of the starting population is assigned a randomly selected location inside the search space according to Eqs.20 - 22.

$$Rb_i = X_b + \text{rand}(1, \text{dim}) * [Y_b - X_b], i = 1 : N_{rb} \quad (20)$$

$$NRb_k(itr+1) = Pb_i + (Pb_k - Pb_j) * X_m + Nds * \text{rand}\left(\frac{1}{2}\left(\frac{5}{100} + r_l\right)\right) \quad (21)$$

$$X_m = c\left(e - e^{\left(\frac{iter-1}{iter_{max}}\right)^2}\right)\sin(2\pi r_2) \quad (22)$$

where iter denotes the current iteration,NRb_k and Rb_k denotes the k^{th} rabbit's previous and current positions: NDS denotes the normal distribution standard function. The flow chart of the ARO based MPPT is represented in Fig.9.

In a subsequent phase, it is feasible to reduce the possibility that an opponent will successfully capture a rabbit by using the randomized concealment technique. Rabbits may endure a lack of energy when they reach the third stage, which could lead them to discontinue their strategy in favor of an unpredictable evading approach. The positions of the rabbits are modified in accordance with each iteration. Eq.21 can be used to mathematically represent the rabbits' detour foraging. A rabbit usually digs many tunnels nearer to its nest to utilize as cover while fending off predators. The formula below is presented.

$$b_{j,k}(iter) = Pb_k(itr) * (1 + C.T) \quad (23)$$

$$k = 1 : N_{Rb} \ \& \ j = 1 : \text{dim} \quad (24)$$

$$C = r_4 \frac{itr_{max} - (itr+1)}{itr_{max}} \quad (25)$$

$$C(j) = \begin{cases} 1, j = k, j = 1 : \text{dim} \\ 0, \text{else} \end{cases} \quad (26)$$

Modeling the transition from the finding phase related to detour foraging to the exploitation phase related to randomized concealment requires a substantial amount of energy. The following factors (AF) can be used to define the energy factor.

$$AF(iter) = 4 * \ln\frac{1}{r}\left(1 - \frac{iter}{iter_{max}}\right) \quad (27)$$

Table 2. Converter specifications

Paramters	Values
C_{in}	100μF
C_{out}	100μF
L	3mH
R_{Load}	30Ω
f_{sw}	10kHz

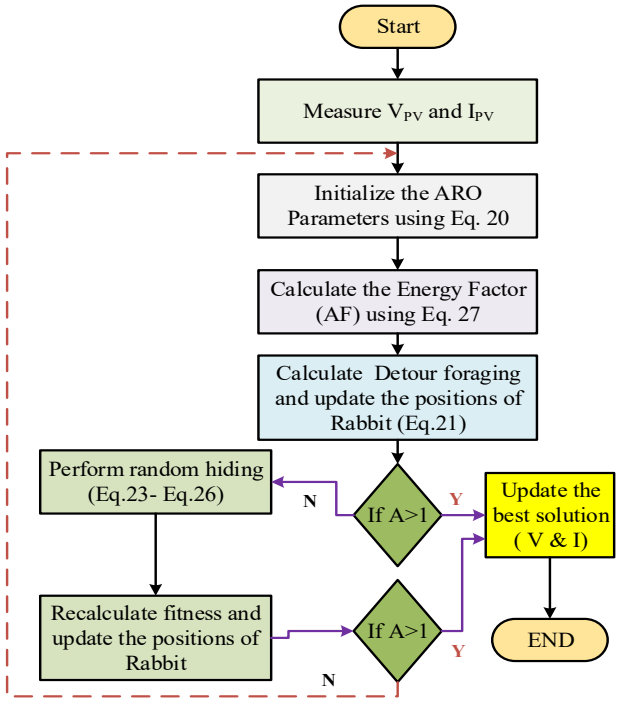

Fig. 9. Flowchart of ARO MPPT.

4. Results and Discussion

Comprehensive simulation analyses have been carried out to assess the reliability of the proposed ARO MPPT algorithm, and the outcome is compared to MPPT algorithms centered around P&O, PSO, FPA, CS, and GWO, based on a variety of attributes under the PS conditions depicted in **Fig. 7** and a constant temperature of 25°c. The first is the GMPPT's capability to converge to the appropriate GMPP. This criterion determines the algorithm's dependability and robustness, making it the most significant one. The second is the maximum time, or the overall time required for reaching the GMPP. The third is the point at which it converges at its highest power. The MPPT efficiency during the change from one shade pattern to another is referred to as the transient efficiency, which comes in at number four. Only the results that are relevant to the important discoveries are presented and tabulated in

Table 3, including the maximum power and numerical values of assessment criteria for all GMPPT techniques.

The PV system employed in this study is shown in Fig. 4. It is made up of a PV array, a dc-dc converter, a dc load, and an appropriate metahurestic MPPT control method.

Table **2** contains a list of the various system parameters.

Table 3. Performance evaluations of MPPT techniques

MPPT Technique	Parameters								
	Pmax (W)	Mean	Median	Standard Deviation (std)	Root Mean Square (RMS)	Rise Time (ms)	Settling Time (s)	Overshoot (%)	Efficency (%)
CS	102	93.1	97.3	14.67	94.67	295.87	1.981	-0.36	97.61%
FPA	104	86.14	84.14	16.34	87.94	104.2	1.966	-	99.52%
GWO	104	90.44	90.44	18.75	92.37	678.08	1.079	-	99.52%
PSO	102.8	93.17	102.0	17.72	94.84	484.11	1.833	-	98.37%
P&O	104	91.52	102.2	20.24	93.73	506.33	1.962	-	99.52%
ARO	104.48	100.4	104.4	13.15	101.3	387.37	2.77	0.441	99.98%

According to Table 3, the ARO-based MPPT approach surpasses all other MPPT techniques while monitoring the GMPP of 104.5 watts. With respect to certain performance measures, it has a mean of 100.4, a median of 104.4, and a standard deviation of 13.15. With the lowest rise time of 387.37 ms, a settling time of 2.27 seconds, the lowest overshoot of 0.441%, and an efficiency of 99.98%, it can be deemed an effective means to handle PS conditions in PV systems which are evident form the results depicted in Fig.10 while the comparative analysis of the various parameters used for evaluation are represented in Fig.12 , while the comparative analysis of MPPT is represented in Fig.11. Fig.10 displays the simulation results for each algorithm discussed in relation to GMPP tracking, PV voltage and current, and duty cycle control.

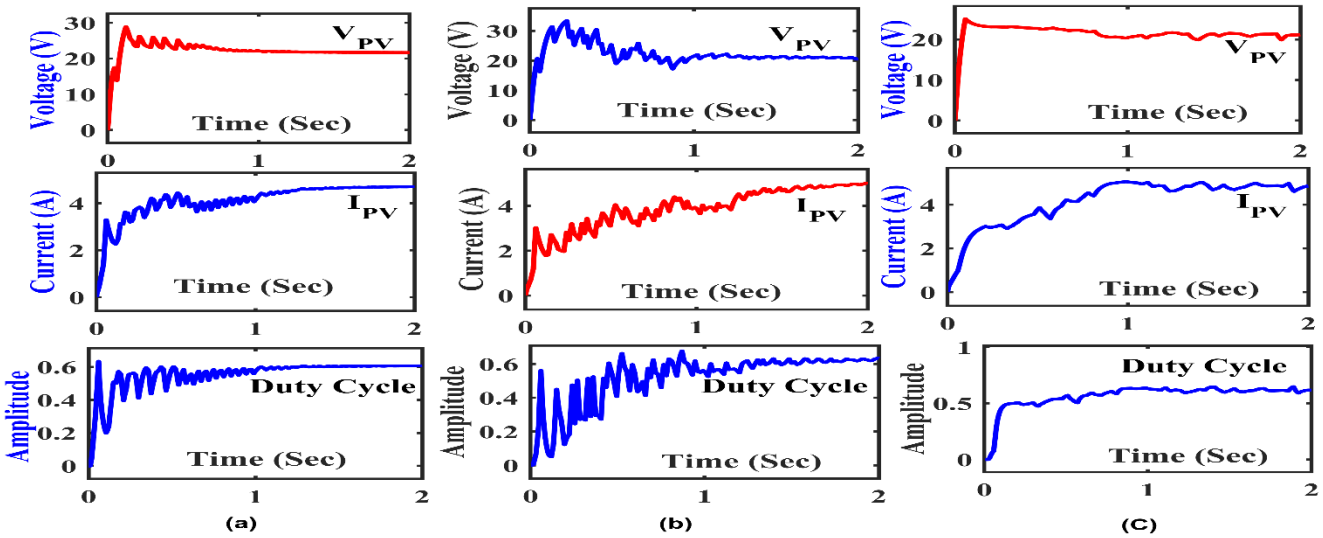

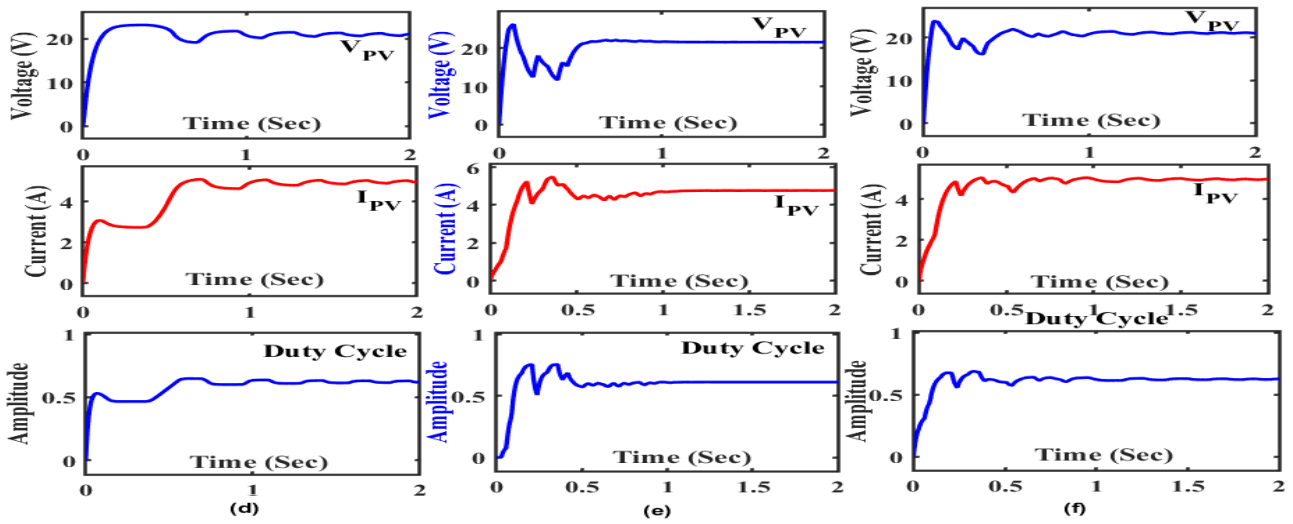

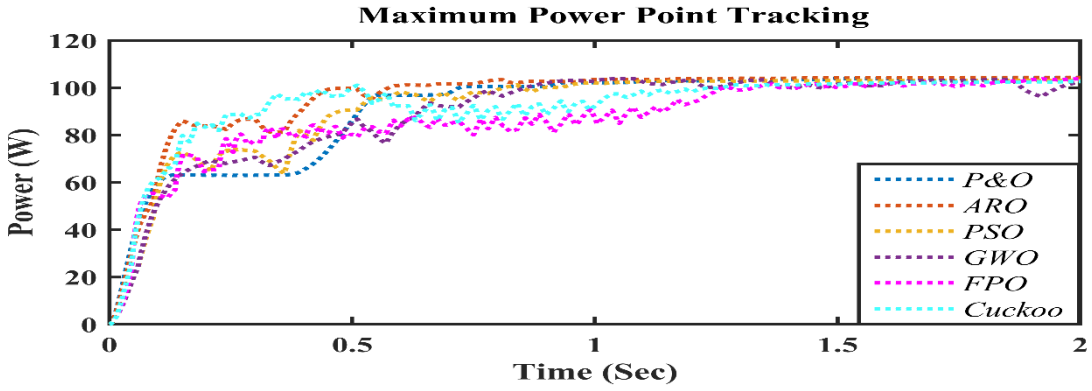

(g)

Fig. 10. Voltage , current and duty cycle control using
(a) CS , (b) FPA, (c) GWO, (d) PO and (e) PSO (f) ARO (g) Comparative analysis of MPPT.

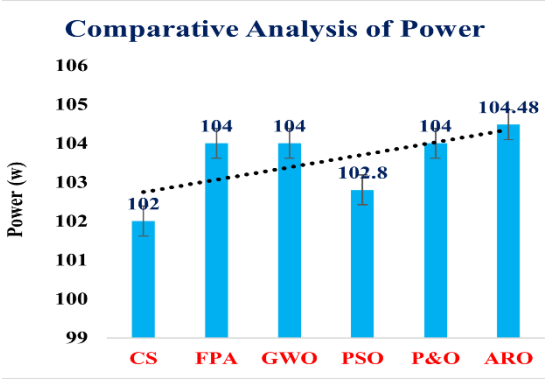

Fig. 11. Comparitive analysis of power.

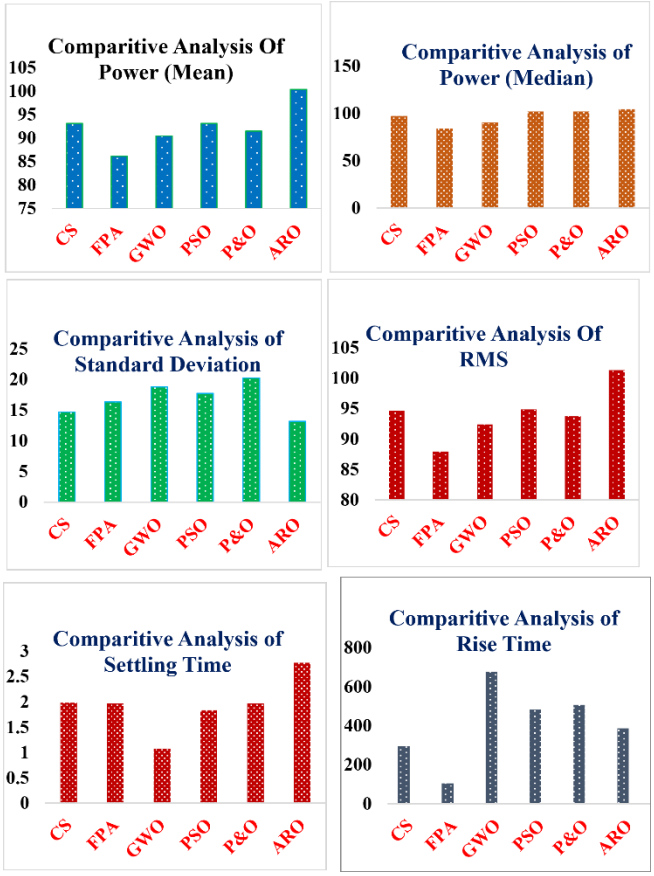

Fig. 12. Comparative analysis of

Table 3 parameters.

5. Limitation and Future Scope

Identifying an optimization method can be challenging due to the abundance of possibilities, and many of them lack a mathematical foundation. Reconfiguring photovoltaic (PV) module interconnections to minimize loops is tricky. Some optimization methods struggle to avoid local hotspots and track LMPP in place of GMPP in solar PV modules. Novel optimization needs to concentrate on accuracy, estimation time, and real-time execution. The integration of machine learning, deep learning, and artificial intelligence represents the latest innovations applicable to the field of PV systems. Considering these advancements is crucial when developing novel algorithms to address the diverse challenges faced by PV systems. These developments have the potential to enhance the adaptive capabilities of PV systems, allowing for real-time performance optimization based on irradiation and temperature data. This integration is considered the future scope, alongside hardware implementation for validating the presented results.

6. Conclusion

In order to extract the most power possible from a PV array working under PSCs, a new MPPT controller based on the ARO metaheuristic algorithm is presented and discussed in this paper. For a 104.5 W PV system, the suggested ARO-based MPPT method has been provided and put into practice using the MATLAB/SIMULINK platform. Additionally, this study did a performance comparison assessment of the proposed MPPT method versus well-known existing MPPT methods, including GWO, PSO, FPA, CA, and P&OThe simulation results under various partial shade conditions demonstrate the new ARO-based MPPT method's significant advantages over existing approaches (GWO, PSO, FPA, CS, and P&O) in terms of tracking reliability, rate of convergence to GMPP, and various other parameters listed in

Table 3. The key findings are discussed below, which are also evident from the comparative analysis shown in Table 3 and through Figs. 11 -

Fig. 12.

- Reduced oscillations with a 0.44% peak overshoot .
- Significantly better mean power with 104 w and a standard deviation of 13.15.
- The Pmax, mean, and median for CS were 102W, 93.1W, and 97.3W, respectively. The RMS was 94.67 W, while the standard deviation was 14.67 W. The rising and settling periods were, respectively, 295.87 s and 1.981 ms.
- The FPA algorithm's Pmax was 104W, with a mean of 86.14W and a median of 84.14W. The RMS was 87.94 W, while the SD was 16.34 W. Rise time was 104.2 ms, and settling time was 1.966 ms.
- The mean and median values for the GWO algorithm are 90.44W and 104W, respectively. RMS was 92.37 W, and the standard deviation was 18.75 W. The rise time was 678.08 ms, and the settling time was 1.079 s.
- Pmax, mean, and median values for the PSO algorithm were 102.8 W, 93.17 W, and 102.8 W, respectively. The RMS was 94.84 W, and the standard deviation was 17.72 . Rise time was 484.11 ms, and settling time was 1.833 ms.
- The Pmax is 104 W, the mean is 91.52 W, and the median is 102.2 W for the P&O algorithm. The RMS was 93.73 W, and the standard deviation was 20.24 W. Rise time was 506.33 ms, while settling time was 1.962 ms.
- The Pmax, mean, and median values for the ARO algorithm were 104.48W, 100.4W, and 104.4W, respectively. With an RMS of 101.3W, the standard

deviation was 13.15W. The rise time was 387.37 ms, and the settling time was 2.77 ms. There was a 0.441% overshoot.

Nomenclature:

PV	Photovoltaic
GMPP	Global maximum power point
LMPP	Local maximum power point
PS	Partial shading
P&O	Perturb and observe
FPA	Flower pollination algorithm
FSSO	Flying Squirrel Search Optimization
ARO	Artificial rabbit optimization
GWO	Grey wolf optimization
PSO	Particle swarm optimization
IC	Incremental conductance
MPP	Maximum power point
CS	Cuckoo Search
G	Irradiation
T	Temperature
MPPT	Maximum power tracking
GMPPT	Global Maximum point tracking

Acknowledgements

The authors would like to express their sincere gratitude to Shivalik College of Engineering and UPES Dehradun for providing academic support, resources, and a conducive research environment for carrying out this work.

Their encouragement and institutional facilities greatly contributed to the successful completion of this research study.

Author Contributions

NKP: Conceptualization, Methodology, Writing – original draft, Software, Visualization. **RKP**: Methodology, Data curation, Writing – review and editing, supervision. **SC:** Investigation, review and editing, supervision. **SBT**: Supervision, Writing–review and editing. **SKM**: Formal analysis, Resources, review and editing**. RY**: Visualization, Writing – review and editing.

Conflict of Interest statement

The authors declare that there is no conflict of interest regarding the outcomes of the study.

References

[1] R. K. Pachauri, "Imperative role of optimization techniques to reconfigure solar photovoltaic array systems to diminish shading effects," Int. J. Circuit Theory Appl., vol. 50, no. 1, pp. 317–353, 2022, doi:10.1002/cta.3152.

[2] N. Kumar, I. Hussain, B. Singh, and B. K. Panigrahi, "Framework of maximum power extraction from solar PV panel using self predictive perturb and observe algorithm," IEEE Trans. Sustain. Energy, vol. 9, no. 2, pp. 895–903, 2018, doi:10.1109/TSTE.2017.2764266.

[3] X. Ge, F. W. Ahmed, A. Rezvani, N. Aljojo, S. Samad, and L. K. Foong, "Implementation of a novel hybrid BAT-fuzzy controller based MPPT for grid-connected PV-battery system," Control Eng. Pract., vol. 98, p. 104380, 2020, doi:10.1016/j.conengprac.2020.104380.

[4] P. Verma, R. Garg, and P. Mahajan, "Asymmetrical interval type-2 fuzzy logic control based MPPT tuning for PV system under partial shading condition," ISA Trans., vol. 100, pp. 251–263, 2020, doi:10.1016/j.isatra.2020.01.009.

[5] V. Srinivasan, C. S. Boopathi, and R. Sridhar, "A new meerkat optimization algorithm based maximum power point tracking for partially shaded photovoltaic system," Ain Shams Eng. J., vol. 12, no. 4, pp. 3791–3802, 2021, doi:10.1016/j.asej.2021.03.017.

[6] M. Mao, L. Cui, Q. Zhang, K. Guo, L. Zhou, and H. Huang, "Classification and summarization of solar photovoltaic MPPT techniques: A review based on traditional and intelligent control strategies," Energy Rep., vol. 6, pp. 1312–1327, 2020, doi:10.1016/j.egyr.2020.05.013.

[7] J. Ahmed and Z. Salam, "A maximum power point tracking (MPPT) for PV system using cuckoo search with partial shading capability," Appl. Energy, vol. 119, pp. 118–130, 2014, doi:10.1016/j.apenergy.2013.12.062.

[8] X. Ge, F. W. Ahmed, A. Rezvani, N. Aljojo, S. Samad, and L. K. Foong, "Implementation of a novel hybrid BAT-fuzzy controller based MPPT for grid-connected PV-battery system," Control Eng. Pract., vol. 98, p. 104380, 2020, doi:10.1016/j.conengprac.2020.104380.

[9] C. B. Pop, T. D. Cioara, I. Anghel, I. Salomie, M. Antal, and R. F. Babiceanu, "Review of bio-inspired optimization applications in renewable-powered smart grids: Emerging population-based metaheuristics," Energy Rep., vol. 8, pp. 11769–11798, 2022, doi:10.1016/j.egyr.2022.09.025.

[10] S. Motahhir, A. El Hammoumi, and A. El Ghzizal, "The most used MPPT algorithms: Review and the suitable low-cost embedded board for each algorithm," J. Clean. Prod., vol. 246, p. 118983, 2020, doi:10.1016/j.jclepro.2019.118983.

[11] S. Titri, C. Larbes, K. Y. Toumi, and K. Benatchba, "A new MPPT controller based on the ant colony optimization algorithm for photovoltaic systems under partial shading conditions," Appl. Soft Comput., vol. 58, pp. 465–479, 2017, doi:10.1016/j.asoc.2017.05.017.

[12] S. Mohanty, B. Subudhi, and P. K. Ray, "A new MPPT design using grey wolf optimization technique for photovoltaic system under partial shading conditions," IEEE Trans. Sustain. Energy, vol. 7, no. 1, pp. 181–188, 2016, doi:10.1109/TSTE.2015.2482120.

[13] R. Motamarri, N. Bhookya, and B. Chitti Babu, "Modified grey wolf optimization for global maximum

power point tracking under partial shading conditions in photovoltaic system," Int. J. Circuit Theory Appl., vol. 49, no. 7, pp. 1884–1901, 2021, doi:10.1002/cta.3018.

[14] M. A. Mohamed, A. A. Zaki Diab, and H. Rezk, "Partial shading mitigation of PV systems via different meta-heuristic techniques," Renew. Energy, vol. 130, pp. 1159–1175, 2019, doi:10.1016/j.renene.2018.08.077.

[15] K. Ishaque and Z. Salam, "A deterministic particle swarm optimization maximum power point tracker for photovoltaic system under partial shading condition," IEEE Trans. Ind. Electron., vol. 60, no. 8, pp. 3195–3206, 2013, doi:10.1109/TIE.2012.2200223.

[16] K. Sundareswaran, S. Peddapati, and S. Palani, "MPPT of PV systems under partial shaded conditions through a colony of flashing fireflies," IEEE Trans. Energy Convers., vol. 29, no. 2, pp. 463–472, 2014, doi:10.1109/TEC.2014.2298237.

[17] N. Singh, K. K. Gupta, S. K. Jain, N. K. Dewangan, and P. Bhatnagar, "A flying squirrel search optimization for MPPT under partial shaded photovoltaic system," IEEE J. Emerg. Sel. Top. Power Electron., vol. 9, no. 4, pp. 4963–4978, 2021, doi:10.1109/JESTPE.2020.3024719.

[18] M. Kermadi, Z. Salam, J. Ahmed, and E. M. Berkouk, "An effective hybrid maximum power point tracker of photovoltaic arrays for complex partial shading conditions," IEEE Trans. Ind. Electron., vol. 66, no. 9, pp. 6990–7000, 2019, doi:10.1109/TIE.2018.2877202.

[19] B. Babes, A. Boutaghane, and N. Hamouda, "A novel nature-inspired maximum power point tracking controller based on ACO-ANN algorithm for photovoltaic system fed arc welding machines," Neural Comput. Appl., vol. 34, no. 1, pp. 299–317, 2022, doi:10.1007/s00521-021-06393-w.

[20] B. Babes, A. Boutaghane, N. Hamouda, S. Kahla, and A. Beddar, "New optimal control of permanent magnet DC motor for photovoltaic wire feeder systems," J. Eur. Syst. Autom., vol. 53, no. 6, pp. 811–823, 2020, doi:10.18280/jesa.530607.

[21] N. Hamouda, B. Babes, S. Kahla, A. Boutaghane, A. Beddar, and O. Aissa, "ANFIS controller design using PSO algorithm for MPPT of solar PV system powered brushless DC motor based wire feeder unit," Proc. Int. Conf. Electr. Eng. (ICEE), 2020, doi:10.1109/ICEE49691.2020.9249869.

[22] N. Hamouda, B. Babes, S. Kahla, Y. Soufi, J. Petzoldt, and T. Ellinger, "Predictive control of a grid connected PV system incorporating active power filter functionalities," Proc. Int. Conf. Sustain. Renew. Energy Syst. Appl. (ICSRESA), pp. 1–5, 2019, doi:10.1109/ICSRESA49121.2019.9182655.

[23] S. Motahhir, S. Chtita, A. Chouder, and A. El Hammoumi, "Enhanced energy output from a PV system under partial shaded conditions through grey wolf optimizer," Clean Eng. Technol., vol. 9, p. 100533, 2022, doi:10.1016/j.clet.2022.100533.

[24] X. S. Yang, "Flower pollination algorithms," in Nature-Inspired Optimization Algorithms, Elsevier, 2014, pp. 155–173, doi:10.1016/b978-0-12-416743-8.00011-7.

[25] S. Mirjalili, S. M. Mirjalili, and A. Lewis, "Grey wolf optimizer," Adv. Eng. Softw., vol. 69, pp. 46–61, 2014, doi:10.1016/j.advengsoft.2013.12.007.

[26] X. Yang and S. Deb, "Cuckoo search via Lévy flights," Proc. IEEE World Congr. Nature Biol. Inspired Comput., pp. 210–214, 2009.

[27] A. F. Mirza, M. Mansoor, and Q. Ling, "A novel MPPT technique based on Henry gas solubility optimization," Energy Convers. Manag., vol. 225, p. 113409, 2020, doi:10.1016/j.enconman.2020.113409.

[28] L. Wang, Q. Cao, Z. Zhang, S. Mirjalili, and W. Zhao, "Artificial rabbits optimization: A new bio-inspired meta-heuristic algorithm for solving engineering optimization problems," Eng. Appl. Artif. Intell., vol. 114, p. 105082, 2022, doi:10.1016/j.engappai.2022.105082.